



1 **Expression of the “4.2 ka event” drought in the southern**
2 **Rocky Mountains, USA**

3

4

5 David T. Liefert¹, Bryan N. Shuman¹

6 1) Department of Geology and Geophysics, University of Wyoming, Laramie, WY 82070, USA

7

8

9

10

11

12

13

14

15

16

17

18

19

20

21

22

23

24 *Correspondence to:* David T. Liefert (dliefert@openspace.org)



25 **Abstract**

26 The use of the climatic anomaly known as the “4.2 ka event” as the stratigraphic division
27 between the mid- and late Holocene has prompted debate over its impact, geographic pattern,
28 and significance. The anomaly has primarily been described as abrupt drying, but evidence of
29 hydroclimate change at ca. 4 ka is inconsistent among sites globally, and few sites in North
30 America document a major drought. Climate records from the southern Rocky Mountains
31 demonstrate the challenge with diagnosing the extent and severity of the anomaly. Dune-field
32 chronologies and a pollen record in southeast Wyoming reveal several centuries of low moisture
33 at around 4.2 ka and prominent low stands in lakes in Colorado suggest the drought was unique
34 amid Holocene variability, but detailed carbonate oxygen isotope ($\delta^{18}\text{O}_{\text{carb}}$) records from
35 Colorado do not record it. We find new evidence from $\delta^{18}\text{O}_{\text{carb}}$ in a small mountain lake in
36 southeast Wyoming of an abrupt reduction in effective moisture or snowpack from
37 approximately 4.2–4 ka that coincides in time with the other evidence from the southern Rocky
38 Mountains and the western Great Plains of regional drying at around 4.2 ka. We find that the
39 $\delta^{18}\text{O}_{\text{carb}}$ in our record may reflect cool-season inputs into the lake, which do not appear to track
40 the strong enrichment of heavy oxygen by evaporation during summer months today. The
41 modern relationship differs from some widely applied conceptual models of lake-isotope systems
42 and may indicate reduced winter precipitation rather than enhanced evaporation at ca. 4.2 ka.
43 Inconsistencies among the North American records, particularly in $\delta^{18}\text{O}_{\text{carb}}$ trends, thus show that
44 site-specific factors can prevent identification of the patterns of multi-century drought. However,
45 the prominence of the drought at ca. 4 ka among a growing number of sites in the North
46 American interior suggests it was a regionally substantial climate event amid other Holocene
47 variability.



48 **1. Introduction**

49 Rapid climate changes are well documented in the late Pleistocene and early Holocene,
50 such as during the Younger Dryas chronozone and at 8.2 ka (thousands of years before present;
51 Alley et al., 1997; Clark et al., 1999; Von Grafenstein et al., 1998), but mid- to late-Holocene
52 changes are less well understood (Wanner et al., 2008, 2011). One potential abrupt change
53 during this time, a multi-century climatic anomaly known as the “4.2 ka event,” has been used
54 as the benchmark for the stratigraphic division between the mid- and late Holocene (Walker et
55 al., 2019). Consequently, the 4.2 ka event has become a topic of scrutiny with debate over its
56 impact, geographic pattern, and significance (Bradley & Bakke, 2019; Weiss, 2016, 2019). The
57 ostensibly global event has primarily been described as a dry episode at low and mid-latitudes
58 (Booth et al., 2005; Nakamura et al., 2016; Di Rita & Magri, 2019; Scuderi et al., 2019; Xiao et
59 al., 2018). Consistent with spatial variation expected from climate variability that shifts
60 atmospheric waves and dynamics, however, some regions show increased precipitation (Huang
61 et al., 2011; Railsback et al., 2018) or no change (Roland et al., 2014).

62 Despite the widespread examination of the 4.2 ka event, its cause and significance amid
63 other millennial-to-centennial climate variability during the Holocene remain unknown. Recent
64 simulations have produced similar patterns of extended drought in the northern hemisphere
65 without external forcings such as insolation changes or volcanism (Yan & Liu, 2019), and others
66 confirm that multi-decadal megadroughts can arise through internal climate variability without
67 changes in boundary conditions (Ault et al., 2018). Internal climate dynamics and feedbacks
68 could also interact with stochastic variability and external forcing to produce such events without
69 consistent or linear relationships to the forcing; forcing may only have a modest probability of



70 triggering rapid climate changes (Renssen et al., 2006). Less clear is how unusual or frequent
71 prolonged ‘megadroughts’ may be within the Holocene across different regions.

72 That such droughts can occur stochastically indicates the 4.2 ka event could be an
73 example of typical late-Holocene climate variability at multi-century time scales (Shuman &
74 Burrell, 2017), but in at least some regions, the event may be exceptional within the spectrum of
75 Holocene variability. Evidence for a major hydroclimate change at ca. 4 ka has been growing in
76 the North American midcontinent (Booth et al., 2005; Carter et al., 2018; Dean, 1997; Denniston
77 et al., 1992; Halfen & Johnson, 2013; Jiménez-Moreno et al., 2019), and adjacent regions, such
78 as the northeastern United States, where it is recorded as part of a series of Holocene wetting and
79 drying events (Newby et al., 2014; Shuman et al., 2019; Shuman & Burrell, 2017). The event’s
80 significance or uniqueness has been difficult to verify, however, in North America where few
81 sites document the anomaly compared to other regions of the mid-latitudes globally (Ran &
82 Chen, 2019; Zhang et al., 2018).

83 Records from the southern Rocky Mountains demonstrate the challenge. In the mid-
84 latitude Rocky Mountains, only dune and pollen records have been explicitly interpreted to show
85 the 4.2 ka event. Initial recognition in North America derived from the timing of the reactivation
86 of the Ferris, Seminoe, and Casper Dune Fields in east-central Wyoming (Fig. 1; Booth et al.,
87 2005; Halfen et al., 2010; Stokes & Gaylord, 1993), but the extent of the drought has been
88 unclear because other dune-field chronologies in the adjacent western Great Plains do not clearly
89 document the drought (Dean, 1997; Halfen & Johnson, 2013; Mason et al., 1997). More recently,
90 Carter et al. (2013, 2017a, 2018) used fossil pollen from Long Lake in the Medicine Bow
91 Mountains, south of the Wyoming dune fields (Fig. 1), to identify a 150-year interval of
92 increased temperature and decreased precipitation centered at 4.2 ka. The inferred precipitation



93 reductions were largest in springtime (Carter et al., 2018), when snowfall in the southern Rocky
94 Mountains is highest today (Mock, 1996). Consistent with this interpretation, prominent
95 stratigraphic evidence of lake-level changes in Colorado and Wyoming lakes could indicate that
96 low water phases at ca. 4.2 ka were one of the most prominent hydrologic changes during the
97 Holocene (Jiménez-Moreno et al., 2019; Shuman et al., 2009; Shuman et al., 2014, 2015). It
98 stands out as one of the only multi-centennial features in a summary of low lakes in the Rocky
99 Mountains during the late-Quaternary (Shuman and Serravezza 2017).

100 By contrast, the 4.2 ka event does not appear in stable oxygen isotope records from lakes
101 in the same region, such as detailed carbonate- $\delta^{18}\text{O}$ ($\delta^{18}\text{O}_{\text{carb}}$) records from Bison and Yellow
102 lakes, Colorado (Fig. 1; Anderson, 2011, 2012). Widely applied conceptual models of lake-
103 isotope systems indicate that hydrologic controls on isotope budgets and the timing of carbonate
104 formation should play an important role in how the event was recorded, but that the isotopic
105 response should vary predictably by hydrologic setting (e.g., Anderson et al., 2016; Leng &
106 Marshall, 2004; Talbot, 1990). According to such models, long lake-water residence times and
107 high rates of evaporation cause hydrologically closed lakes (i.e., terminal basins) to record shifts
108 in effective moisture (precipitation – evaporation) because endogenic carbonates will typically
109 precipitate in evaporated, ^{18}O -rich water during the warm summer months. Drought could affect
110 such a lake-isotope system by both increasing evaporation and changing seasonal precipitation,
111 such as by reducing snowpack. In hydrologically open lakes with short residence times, the
112 continual replacement of evaporated water creates isotopic sensitivity primarily to the seasonal
113 balance of precipitation without a strong evaporation effect. Many lakes fall somewhere between
114 fully hydrologically open and closed and additional site-specific influences may also override
115 such expectations. Consequently, not all stable oxygen isotope records from lakes may have been



116 sensitive to the specific climate variables that changed at 4.2 ka. Modern lake-water
117 measurements can help to identify the relative influences of different controls (Fig. 2; Anderson
118 et al., 2016).

119 Here we present a new $\delta^{18}\text{O}_{\text{carb}}$ record from Highway 130 Lake (HL) in southeast
120 Wyoming near where other Holocene paleohydrological and paleoecological records have been
121 developed (Mensing et al., 2012; Minckley et al., 2012; Brunelle et al., 2013). HL is an
122 intermittently closed subalpine lake in the Medicine Bow Mountains, within 20 km of Long Lake
123 where fossil pollen indicates a prolonged ‘megadrought’ at 4.2 ka (Fig. 1; Carter et al., 2018).
124 The lake is also <60 km from Upper Big Creek Lake, Colorado, where a prominent
125 paleoshoreline detected in geophysical surveys and cores indicates low water after 4.7 ka (Fig. 1;
126 Shuman et al., 2015). Previous work at HL indicates a strong influence of evaporation on the
127 lake and its water isotopes, which we compare with Bison and Yellow lakes in Colorado (Fig. 2;
128 Liefert et al., 2018). We discuss how dissimilarities in $\delta^{18}\text{O}_{\text{carb}}$ among lakes, possibly driven by
129 non-climatic factors, could complicate interpretations of the patterns of past hydroclimate
130 changes including megadroughts and Holocene trends. Together these outcomes may clarify the
131 timescales on which drought operates within a critical headwater area of North America, but also
132 confirm that interpretations of stable isotope records of past hydroclimate changes may depend
133 heavily on site-specific dynamics.

134

135 2. Site description

136 HL (41°21′05″ N, 106°15′50″ W; 3,199 m a.s.l. (above sea level)) fills a shallow
137 depression in the uneven terrain covering the Libby Creek watershed (12 km² surface area) in the
138 Snowy Range, a southwest trending subsection of the Medicine Bow Mountains in southeast



139 Wyoming (Fig. 1). Around HL, subalpine coniferous forests interspersed with open meadows
140 grow on thin glaciated soils and tills between the frequent outcroppings of the underlying
141 siliceous metadolomite (Houston & Karlstrom, 1992; Musselman et al., 1992). Southeast
142 Wyoming has a semi-arid climate, but high elevations in the Medicine Bow Mountains receive
143 about 1,000 mm of precipitation each year, with approximately 70% of annual totals falling as
144 snow from October to June (Mock, 1996). Local average wind speeds are high (~5 m/s) and
145 minimum winter and maximum summer temperatures typically reach -23°C and 21°C,
146 respectively.

147 The surface watershed around HL occupies ~0.45 km², while the lake has a surface area
148 of ~0.02 km², a maximum (spring) water depth of ~200 cm, and declines in water level by ~30
149 cm from July to late October (Liefert et al., 2018). Ice covers HL from approximately October to
150 May and stream connections shut off in June following spring flooding. Measurements reveal no
151 thermal stratification because of the shallow water depth, flat-bottom bathymetry, and high
152 average wind speeds, which promote mixing throughout the water column (Bello & Smith, 1990;
153 Stewart & Rouse, 1976). Liefert et al. (2018) found that evaporation could account for as much
154 as 83% of the seasonal water loss at HL, though the stable water level and temperature compared
155 to nearby lakes of similar size and depth indicates shallow groundwater flow-through driven by
156 seasonal precipitation and infiltration (Rautio & Korkka-Niemi, 2011; Rosenberry & LaBaugh,
157 2008).

158

159 3. Methods

160 To measure the modern oxygen and hydrogen isotope compositions of the lake water
161 ($\delta^{18}\text{O}$ and δD , respectively) and specific conductance, water samples were collected at

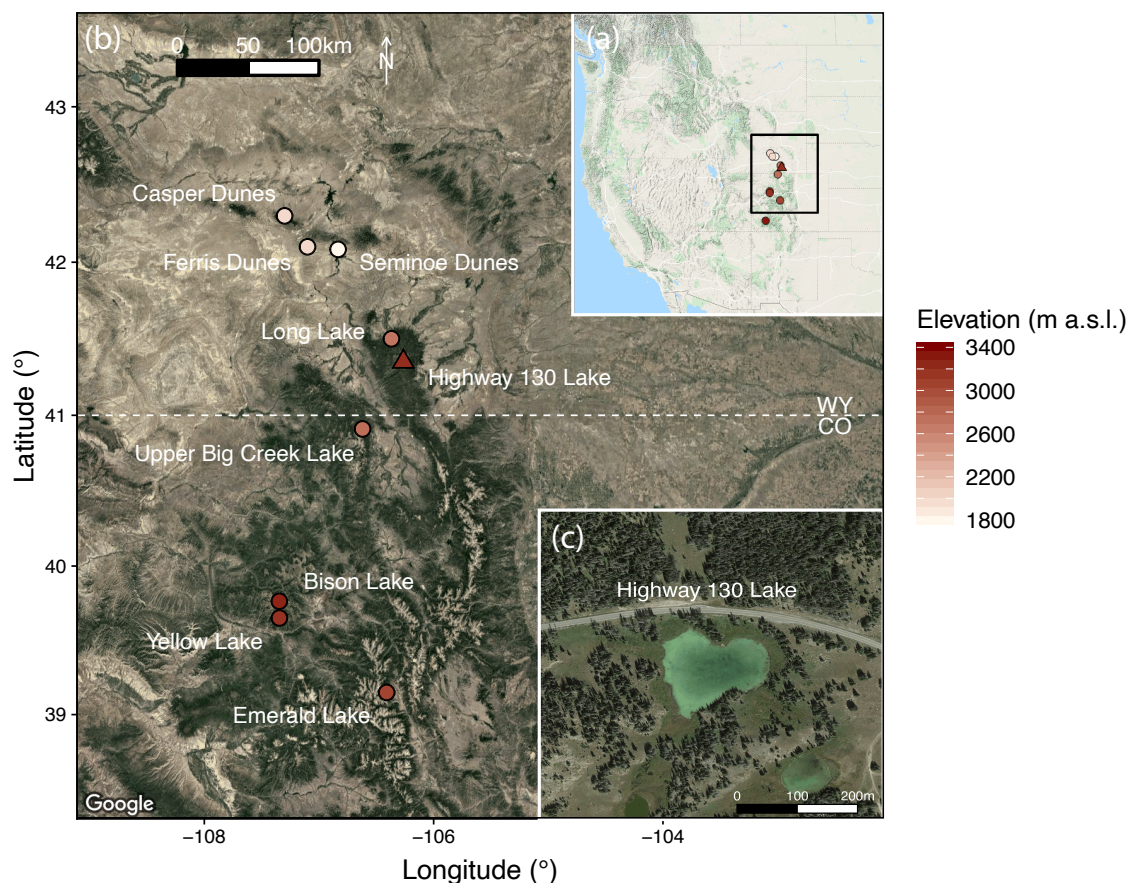


Figure 1. Locations of study site and related climate records. (a), Highway 130 Lake (triangle) and related climate records (circles) lie within the southern Rocky Mountains, a critical headwater area in the western United States that contributes snowmelt to the Colorado and North Platte Rivers. (b), Study site locations in the Colorado Front Range and Medicine Bow Mountains, southeast Wyoming. Little Molas Lake, a comparator site in the inset map (a), lies south of the focal region (b). (c), Highway 130 Lake lies within the Snowy Range, a subsection of the Medicine Bow Mountains. Google images (© Google Maps 2021) were acquired using the ggmap package in R (Kahle & Wickham, 2013).

162 approximately biweekly intervals from June to October in 2017. Additional samples of snowfall,
163 snowpack, rain, and groundwater (from springs and wells) were collected to measure the range in



164 water isotope values of the watershed's hydrologic components. Isotopic ratios were measured at
165 the University of Wyoming Stable Isotope Facility using a Picarro L2130-I Cavity Ring Down
166 Spectrometer and specific conductance was measured using a YSI Multiparameter Water Quality
167 Meter. We acquired meteorological data from SNOTEL stations near HL at Brooklyn Lake,
168 Wyoming (ID 367; 3,121 m a.s.l.; 41.36 °N, -106.23 °W), and at Bison Lake, Colorado (ID 345;
169 3,316 m a.s.l.; 39.76 °N, -107.36 °W), to compare the modern ratios of snow/rain that control the
170 seasonal balance of precipitation at the lakes.

171 In October 2016 we installed a pressure transducer (Onset HOBO U20 Level Data
172 Logger) to measure the water level of HL at 30-min intervals; freezing conditions required that
173 we secure the transducer to the lakebed inside a bladder filled with antifreeze. To compensate for
174 barometric pressure changes we adjusted the transducer data using pressure measurements from
175 the nearby Glacier Lakes Ecosystem Experiments Site Brooklyn Tower Ameriflux site (GLEES
176 Tower; US-GLE: <https://ameriflux.lbl.gov/sites/siteinfo/US-GLE>; 41°21'57" N, 106°14'23" W;
177 3,191 m a.s.l.). In late January 2017, we installed a conductivity data logger (Onset HOBO U24
178 Conductivity Data Logger) at the same location and water depth as the pressure transducer to
179 measure the range in conductivity (converted to specific conductance at 25 °C) at 30-min
180 intervals of the unfrozen water underlying the ice cover to examine the seasonal patterns of water
181 chemistry that influence carbonate formation.

182 At the same time, we collected a 70-mm diameter sediment core with a modified
183 Livingston piston corer from the center of HL where the combined water and ice depth reached
184 approximately 90 cm; we used this depth to calibrate the pressure transducer. The organic and
185 carbonate content of contiguous 1-cm intervals of the sediment core were measured by weighing
186 the residual sediment after burning the samples at 550 and 1000 °C, respectively. One-cm³ sub-



187 samples were isolated from each interval after the 550 °C burn for isotopic analysis to remove
188 organic matter; comparison with organic removal using oxidizing agents indicated no additional
189 fractionation. The sub-samples were also sieved using a 63- μm mesh to isolate the fine fraction
190 for isotopic analysis using a Thermo Gasbench coupled to a Thermo Delta Plus XL isotope ratio
191 mass spectrometer at the University of Wyoming Stable Isotope Facility. X-ray powder
192 diffraction confirmed that the samples contained only calcite. Ostracod tests were present in less
193 than 10 of the 300 samples. We report $\delta^{18}\text{O}_{\text{carb}}$ in the per mil (‰) notation relative to the Vienna
194 Pee Dee Belemnite (VPDB) standard.

195 We isolated sedimentary charcoal ($>125\ \mu\text{m}$) and conifer needles from the sediment core
196 for radiocarbon analyses to estimate sedimentation rates and oxygen isotope chronology
197 calibrated to radiocarbon years using intcal13 (Reimer et al., 2013) and the age-depth model was
198 generated using Bchron (Parnell et al., 2008). Radiocarbon samples were analyzed at the
199 University of California Irvine Keck Carbon Cycle facility.

200

201 4. **Results**

202 4.1 *Modern water-chemistry and level measurements*

203 Lake-water $\delta^{18}\text{O}$ and δD in HL increased during the ice-free season from -17.8‰ and -
204 132‰ (sampled in late June) to -10.8‰ and -94.2‰ (sampled in late October), respectively
205 (black circles, Fig. 2). The local evaporation line (LEL) defined by the HL samples (thick black
206 line, Fig. 2) traces the LEL defined by samples from lakes in the Colorado Front Range (red
207 dashed line, Fig. 2; Henderson & Shuman, 2009). Several consecutive years of measurements
208 reveal that isotope values at HL are consistent from year to year. The LEL's deviation from both
209 the global meteoric water line (GMWL; Fig. 2) and isotope composition of the hydrologic inputs

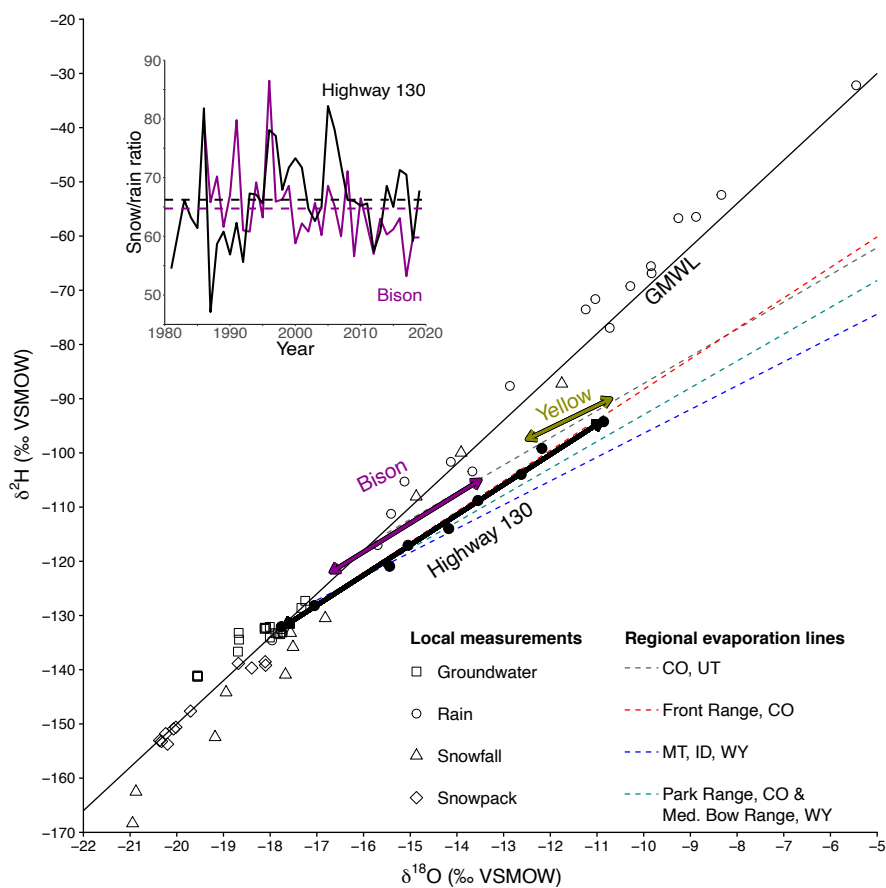


210 (open symbols, Fig. 2) indicates a strong evaporative influence. $\delta^{18}\text{O}$ and δD values at HL also
211 indicate stronger fractionation by evaporation compared to representative warm-season isotope
212 compositions measured at Bison and Yellow lakes (thick purple and yellow lines, Fig. 2;
213 Anderson, 2011, 2012), which remained closer to the composition of meteoric waters. Longer
214 lake-water residence time and higher evaporation in HL thus appear to produce a greater range of
215 warm-season isotope compositions compared to Bison and Yellow Lakes.

216 The different lake-water- $\delta^{18}\text{O}$ values among the lakes contrasts with their similar
217 seasonal precipitation patterns. The modern ratio of snow/rain, which can determine the mean
218 precipitation and lake-water $\delta^{18}\text{O}$, is comparable in the watersheds of HL and Bison Lake (inset
219 plot, Fig. 2). Other modern differences among the lakes, which all have surface areas of < 0.1
220 km^2 , include that the maximum water depth of HL is several meters shallower than Bison and
221 Yellow Lakes (Anderson, 2012) and that the summer lake-water temperatures in HL typically
222 range from 8–12 °C, which is cooler than the epilimnion at Yellow Lake (Anderson, 2012). HL
223 is also several degrees cooler than nearby lakes also without thermal stratification (Liefert et al.,
224 2018).

225 Continuous measurements of specific conductance began in early February when the
226 combined water and ice depth reached approximately 90 cm (Fig. 3). Specific conductance
227 increased from 700 $\mu\text{S}/\text{cm}$ to 1,115 $\mu\text{S}/\text{cm}$ by early April while the lake surface was frozen. The
228 specific conductance fell below 500 $\mu\text{S}/\text{cm}$ as the lake flooded with snowmelt in early May.
229 Specific conductance ranged from 250–300 $\mu\text{S}/\text{cm}$ after the conductivity data logger was
230 removed in late June and before the lake froze over in the fall, and the water depth stayed
231 between 100–150 cm, which was low compared to previous years.

232



233

Figure 2. Modern measurements of $\delta^{18}\text{O}$ and δD . Regional evaporation lines (dashed lines) intersect the global meteoric water line and represent the linear regression of lake-water isotope compositions in a region (Henderson & Shuman, 2009; Anderson et al., 2016). Isotopic measurements from the study watershed (open symbols) show the range in isotope compositions of hydrologic inputs to Highway 130 Lake from the watershed. Arrows represent the range in modern $\delta^{18}\text{O}$ and δD values of Highway 130 Lake (black), Bison Lake (purple; Anderson, 2011), and Yellow Lake (yellow; Anderson, 2012) throughout the ice-free season, and black dots show the individual measurements at Highway 130 Lake. The inset plot shows the modern annual ratio of snow/rain for the SNOTEL stations nearest Highway 130 Lake (black line) and Bison Lake (purple line) and the dashed lines show the means.

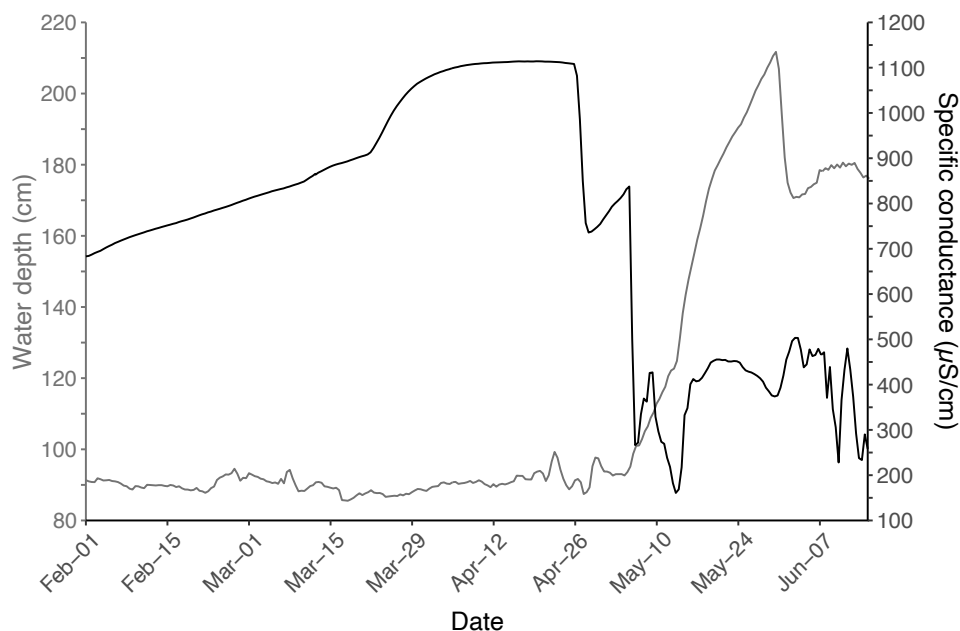


Figure 3. Measurements of water depth (gray line) and specific conductance (black line) at Highway 130 Lake in 2017.

234

235

236 **4.2 Sediment characteristics**

237 The 333-cm core from HL extends to at least the early Holocene and contains
238 predominantly carbonate sediment underlain by silicate clays (Fig. 4). The upper 303 cm
239 contains from 5–55% in organics and 5–90% in carbonate; the core above the basal 30 cm has a
240 mean carbonate content of 65%. In the basal unit, the carbonate content drops below 5%, which
241 was too low for isotopic analysis. The age-depth model (black line with 2-sigma gray uncertainty
242 band, Fig. 4, Table 1) reveals average net sediment accumulation rates of 18 cm/kyr (thousand
243 years) from 11.7–4.4 ka and 45.5 cm/kyr from 4.4 ka to present. High rates of net sedimentation



244 correspond with intervals of high carbonate flux into the lake, indicating that carbonate
 245 production may largely control sedimentation rates. The carbonate content and carbonate flux,
 246 representing the mass of carbonates deposited per unit area per year, increased simultaneously
 247 with the sedimentation rate at 4.4 ka (Fig. 4), but the percent carbonate content subsequently
 248 declined until 4.0 ka. The radiocarbon age at 119-cm depth (3.072 ± 0.03 ka) has an age similar
 249 to the date at 67-cm depth (3.031 ± 0.02 ka), which may indicate a reworked upper age (black
 250 dots in Fig. 4). However, high total sediment and carbonate accumulation rates are inferred even
 251 if the upper age was excluded from the age-depth model.

252

253

254 Table 1. Calibrated radiocarbon ages used for the age-depth model.

Lake	Core	Depth (cm)	Material	Lab number	Age (^{14}C yr BP)	Uncertainty (1σ , ^{14}C yr BP)	Calibrated age ranges (1σ , cal yr BP)		
							Median	Maximum	Minimum
Highway 130 Lake	2A	18	Charcoal	UCIAMS- 194167	850	30	748	783	726
		67	Charcoal	UCIAMS- 194168	2,900	20	3,033	3,070	2,996
	2B	119-121	Charcoal	UCIAMS- 194169	2,925	15	3,073	3,144	3,004
		154-156	Charcoal	UCIAMS- 194170	3,660	35	3,986	4,081	3,921
		193-195	Charcoal	UCIAMS- 194171	3,840	20	4,241	4,290	4,157
		204	Charcoal	UCIAMS- 194172	3,965	20	4,438	4,508	4,412
		239	Charcoal	UCIAMS- 194173	6,210	60	7,096	7,132	7,007
		302	Charcoal	UCIAMS- 194174	9,580	25	10,927	11,074	10,781



255

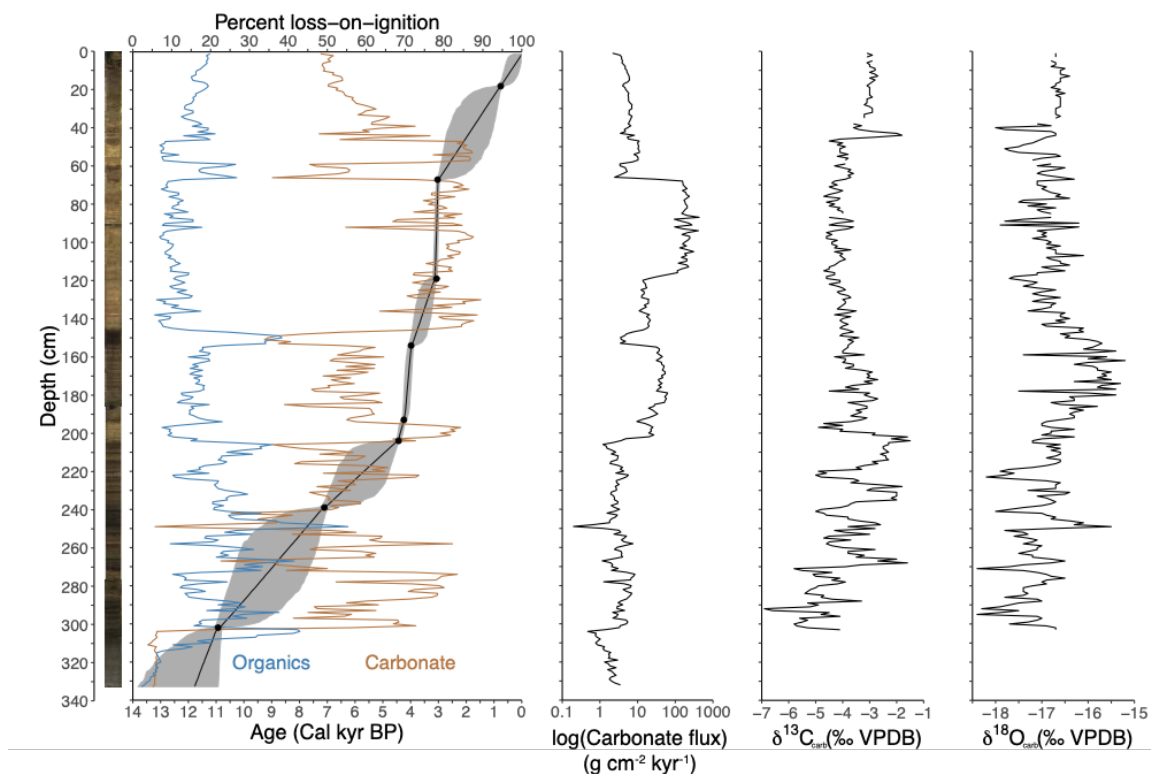


Figure 4. Percent organics, percent carbonate, carbonate flux, $\delta^{13}\text{C}_{\text{carb}}$, and $\delta^{18}\text{O}_{\text{carb}}$ are shown by depth alongside an image of the 333-cm-long sediment core from Highway 130 Lake. Radiocarbon ages (black dots) were used to create the age-depth model and gray uncertainty band (2 sigma).

256

257 *4.3 Sedimentary oxygen and carbon isotopes*

258 $\delta^{13}\text{C}_{\text{carb}}$ and $\delta^{18}\text{O}_{\text{carb}}$ in the upper 303 cm of sediment range from -6.9 to -1.5‰ and -18.4

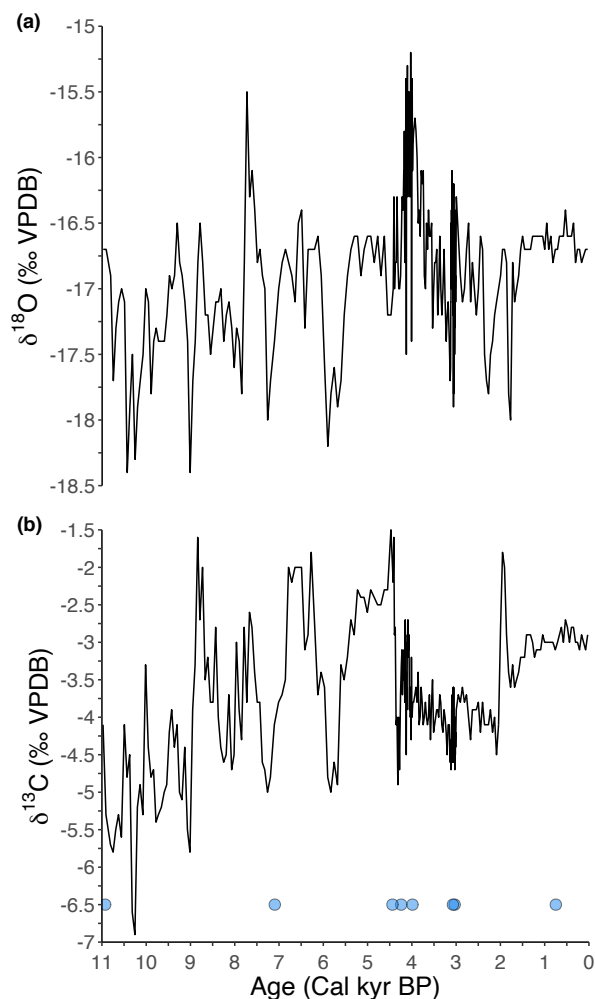
259 to -15.2‰, respectively, and the mean isotope compositions become more positive over the

260 record, but the long-term trend of $\delta^{18}\text{O}_{\text{carb}}$ is not statistically significant (Fig. 4). Variance in

261 $\delta^{13}\text{C}_{\text{carb}}$ and $\delta^{18}\text{O}_{\text{carb}}$ values is highest before 4.4 ka (below 200-cm depth) and lowest since 1.5 ka



262 (above 40-cm depth; Fig. 5). Isotope excursions appear in both the slow and fast sedimentation
263 intervals and when the carbonate flux is both low and high (Fig. 4).



264

Figure 5. $\delta^{18}\text{O}_{\text{carb}}$ (a) and $\delta^{13}\text{C}_{\text{carb}}$ (b) from Highway 130 Lake. The blue dots indicate the calibrated radiocarbon ages used for the age-depth model (refer to Table 1 for calibrated age uncertainties).

265 $\delta^{18}\text{O}_{\text{carb}}$ peaks from approximately 4.2–4 ka, where four calibrated radiocarbon ages
266 constrain the timing and indicate a fast sedimentation rate (Fig. 5). The carbonate flux is high,



267 but the carbonate content is low (~55%) during this interval relative to the mean (Fig. 4). A
268 positive excursion of similar magnitude also occurred from 7.8–7.3 ka, but aligns with high
269 organic content and low $\delta^{13}\text{C}_{\text{carb}}$, carbonate content, carbonate flux, and total net sediment
270 accumulation.
271 Compared to the records for Bison and Yellow Lakes in Colorado (Anderson, 2011, 2012; Fig.
272 1), $\delta^{18}\text{O}_{\text{carb}}$ values of HL are several per mil lower with higher variance for most of the Holocene
273 (Fig. 6). This pattern changes in the late Holocene as carbonate in Bison Lake becomes
274 isotopically lighter than before and approaches the oxygen isotope composition of HL, which
275 maintains a relatively constant mean $\delta^{18}\text{O}_{\text{carb}}$ value. After approximately 1.5 ka, $\delta^{18}\text{O}_{\text{carb}}$
276 variability in HL drops to near the analytical uncertainty ($\pm 0.2\text{‰}$) while the other records show
277 increased variability (Fig. 6).

278

279 5. Discussion

280 5.1 *Evidence of the 4.2 ka drought in the southern Rocky Mountains*

281 Peak $\delta^{18}\text{O}_{\text{carb}}$ in HL indicates an abrupt decline in effective moisture or at least a decline
282 in the ratio of snowfall to rain in the Medicine Bow Mountains from approximately 4.2–4 ka
283 (Fig. 5) when evidence from additional climate records shows that aridity affected the southern
284 Rocky Mountains and portions of the Great Plains (Carter et al., 2013; Halfen & Johnson, 2013;
285 Stokes & Gaylord, 1993). The highest $\delta^{18}\text{O}_{\text{carb}}$ values at HL coincide with the pollen-inferred
286 precipitation and temperature changes at 4.2 ka at Long Lake, which records two centuries of
287 severe drought (Long Lake, Fig. 1; Carter et al., 2013). The excursion also aligns with the

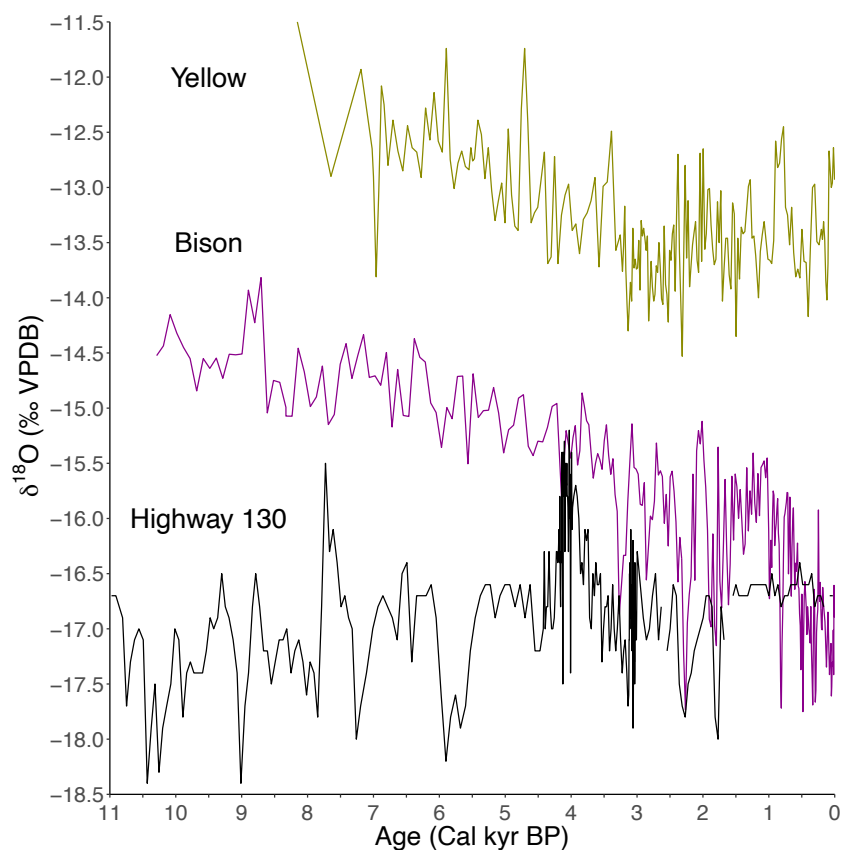


Figure 6. $\delta^{18}\text{O}_{\text{carb}}$ records from Highway 130 Lake (black), Bison Lake (purple; Anderson, 2011), and Yellow Lake (yellow; Anderson, 2012) vary despite their similar locations and elevations.

288 longstanding evidence of drought in the Great Plains and eastern southern Rocky Mountains
289 (dune fields, Fig. 1), where a rapid loss of grain-trapping vegetation likely triggered several
290 centuries of increased aeolian transport documented across multiple dune fields (Booth et al.,
291 2005; Forman et al., 2001; Halfen et al., 2010; Stokes & Gaylord, 1993).

292 Taken together, the records suggest that rapid drying at around 4.2 ka was an important
293 climatic event in the Medicine Bow Mountains even if the drought is not a prominent feature in
294 other paleoclimate studies from the mid-latitude Rocky Mountains (Anderson et al., 2008;



295 Brunelle et al., 2013; Feiler et al., 1997; Johnson et al., 2013; Mensing et al., 2012; Minckley et
296 al., 2012; Shuman et al., 2010; Thompson et al., 1993; Whitlock & Bartlein, 1993), including the
297 nearby $\delta^{18}\text{O}_{\text{carb}}$ records from Bison and Yellow Lakes (Anderson, 2011, 2012). The spatial
298 patterns of late-Holocene hydroclimate changes in North America may have been complex
299 compared to other regions, such as the European continent where late-Holocene climate
300 variability appears more coherently in climate records (e.g., Deininger et al., 2017). Still, the
301 inconsistent evidence complicates interpretations of the 4.2 ka anomaly here and elsewhere
302 (Bradley & Bakke, 2019).

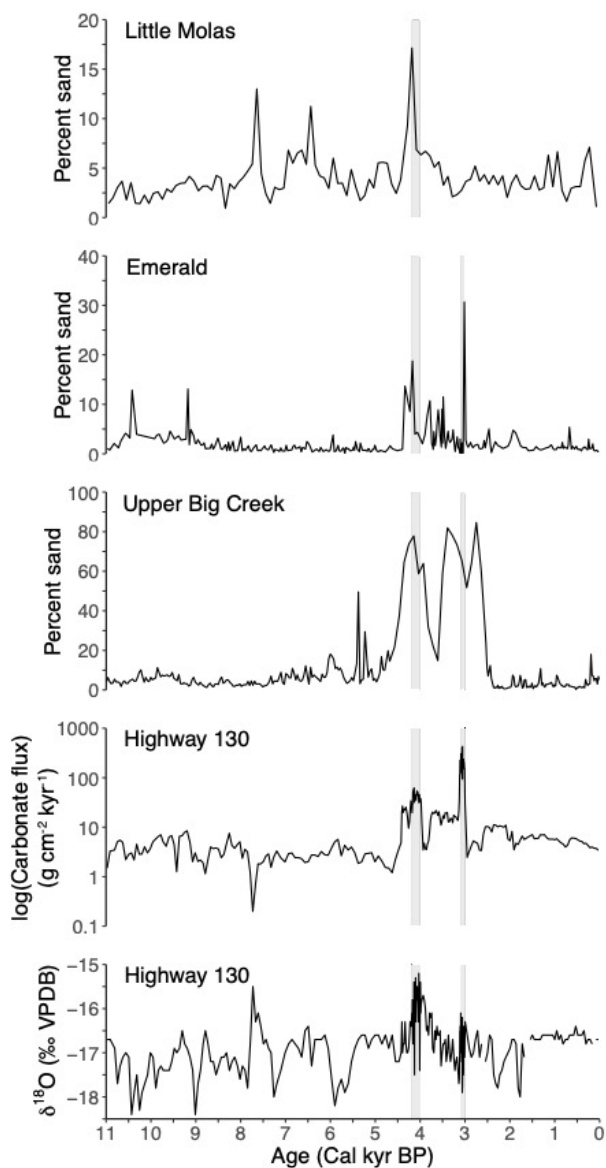
303 Some paleohydrologic evidence indicates, however, that the event may have been
304 extensive in the southern Rocky Mountains. Sedimentological changes in high-elevation lakes in
305 Colorado show substantial hydrological transformation at around 4 ka matching the timing and
306 scale of drought inferred from HL's record (Fig. 1 & 7; Shuman et al., 2009a, 2014, 2015). The
307 sediment stratigraphies record low water levels that shifted shoreline sands to the locations of
308 cores collected in 1–5-m water depth today and thus indicate reduced effective moisture at 4.2–
309 3.9 ka (gray shaded regions, Fig. 7). The sand layers coincide in time with the elevated carbonate
310 accumulation rate and $\delta^{18}\text{O}_{\text{carb}}$ values at HL and with dune activity in southeast Wyoming
311 (Halfen & Johnson, 2013; Stokes & Gaylord, 1993); the high-elevation lake locations and
312 geophysical site surveys confirm that the shallow-water sands were not deposited by aeolian
313 activity. A second prominent sand layer in Emerald and Upper Big Creek Lakes at ca. 3.1 ka
314 (gray shaded regions, Fig. 7) indicates low effective moisture and overlaps with the maximum
315 rate of carbonate accumulation at HL, but a second sand layer does not appear in Little Molas
316 Lake and the $\delta^{18}\text{O}_{\text{carb}}$ values in HL are lower than at 4.2 ka. It took several centuries for $\delta^{18}\text{O}_{\text{carb}}$
317 values to rise and fall before and after the peak from 4.2–4 ka, but the excursion at 3.1 ka



318 occurred within a century. Multiple radiocarbon ages constrain the interval of high carbonate
319 accumulation from approximately 4.4–3 ka, but the sedimentation rate in the interval is sensitive
320 to removal of one of the ages; if the age at ca. 3 ka is out of sequence, we could bias the peak
321 rate of sediment and carbonate accumulation toward high values.

322 The rapid transition from deep-water muds to shallow-water sands as water levels
323 dropped in the Colorado lakes at around 4.2 ka corresponds with changes in pollen assemblages
324 in central Colorado (Jiménez-Moreno et al., 2019) and southeast Wyoming (Carter et al., 2013),
325 as well as with other evidence for drought in North America (Booth et al., 2004). Similar
326 sedimentological features found in lakes along the Atlantic margin from Maine to Pennsylvania
327 date to around 4.2 ka, for example, where the drought appears as one of multiple events linked to
328 circulation changes over the North Atlantic (Li et al., 2007; Marsicek et al., 2013; Newby et al.,
329 2014; Nolan, 2020; Shuman et al., 2019; Shuman & Burrell, 2017). The sequences in the
330 southern Rocky Mountains, however, include uniquely prominent isotopic and sedimentological
331 changes from 4.2–3.9 ka.

332 Given the growing evidence of drought within the southern Rocky Mountains associated
333 with the widespread climatic anomaly at 4.2 ka, a lack of $\delta^{18}\text{O}_{\text{carb}}$ records of the event in the
334 region, or in North America entirely, is surprising (Anderson et al., 2016b; Konecky et al., 2020).
335 However, individual sites respond to a varying mixture of local and regional factors. The
336 stratigraphic evidence of lake-level change in the region is not entirely consistent either and may
337 indicate interactions with different directions of hydroclimate change across seasons, elevations,
338 and latitudes. Stratigraphic features in Hidden Lake, located in northern Colorado just south of
339 Upper Big Creek Lake (Fig. 1) but several hundred meters lower in elevation, document a rapid
340 increase in effective moisture at around 4 ka (Shuman et al., 2009)—the opposite response of the



341

Figure 7. Spikes in the sand content of Little Molas, Emerald, and Upper Big Creek Lakes, located in high-elevation watersheds in Colorado (Fig. 1), align with the positive $\delta^{18}\text{O}_{\text{carb}}$ excursion at Highway 130 Lake and indicate low water from approximately 4.2–4 ka (gray shaded areas) resulting from low effective moisture (Shuman et al., 2009a, 2014, 2015). Another positive $\delta^{18}\text{O}_{\text{carb}}$ excursion at ca. 3.1 ka (gray shaded areas) aligns with intervals of low water at Emerald and Upper Big Creek Lakes.



342 surrounding lakes at higher elevations (Fig. 7). The wet phase was abrupt in onset and
343 termination and lasted from around 4.4–3.7 ka, which stands out in the otherwise gradual trend
344 towards higher water levels since 6 ka without any major intervals of low water in the late
345 Holocene (Shuman et al., 2009).

346 The low-elevation location of Hidden Lake may indicate an important role for increased
347 summer or fall rainfall when high-elevation sites declined in response to low winter snowfall.
348 The combined effects could have favored the unusually high $\delta^{18}\text{O}_{\text{carb}}$ at HL. Low winter snow
349 can create favorable surface-energy conditions for strong summer convective precipitation (Zhu
350 et al. 2005). Alternatively, the reversed hydrologic response of Hidden Lake could indicate
351 antiphased hydroclimate changes in the southern Rocky Mountains between high and low
352 elevations, which is consistent with modern responses to the El Niño-Southern Oscillation
353 (Preece et al., 2020). The active dune fields in east-central Wyoming, however, confound a
354 simple interpretation of the elevational and seasonally antiphased hydrologic changes.
355 Latitudinal hydroclimate variability could be an additional complicating factor and has
356 previously been described across the area due to transient climatic boundaries with the northern
357 and southern Rocky Mountains (Shinker, 2010; Wise, 2010). The comparison of the radiocarbon
358 age uncertainties of the 4.2 ka paleoshoreline sands at lake-level sites, including Emerald Lake in
359 central Colorado (Fig. 1 & 7), indicates a late-Holocene north-south moisture dipole extending
360 across much of the area described here (Shuman et al., 2014).

361 Given the potential prominence of the 4.2 ka drought at HL and other southern Rocky
362 Mountain records, it may have been uniquely severe in this region even if it had a complex
363 regional expression at broader spatial scales. The lake-level reconstructions from Colorado
364 contain evidence of other Holocene hydrologic changes (Fig. 7) and HL shows another positive



365 excursion at 7.8 ka (Fig. 5), but the records lack evidence for multiple recurrent, multi-century
366 hydroclimate changes recorded with the 4.2 ka event in places like the Atlantic margin (Shuman
367 et al., 2019). Elsewhere, aridity at 4.2 ka may represent just one of several repeated drying events
368 consistent with climate records and simulations from around the world that show drought as a
369 regular feature of late-Holocene climate variability (Arz et al., 2006; Bradley & Bakke, 2019;
370 Mayewski et al., 2004; Wanner et al., 2008; Wanner et al., 2015; Yan & Liu, 2019). The mid-
371 latitude Rocky Mountain records may suggest that the midcontinent was insulated from some of
372 the abrupt late-Holocene climate changes, possibly due to its isolation from the ocean-
373 atmosphere dynamics proposed to play key roles in Holocene variability (Arz et al., 2006;
374 Deininger et al., 2017; Jalali et al., 2019; Yan & Liu, 2019).

375

376 **5.2 Varying $\delta^{18}O_{carb}$ trends in the southern Rocky Mountains**

377 The marked sensitivity of lake-water $\delta^{18}O$ to hydroclimate changes may make lacustrine
378 carbonates ideal indicators of past droughts like the 4.2 ka event, as documented by $\delta^{18}O_{carb}$
379 records outside of North America (e.g., Bini et al., 2019; Dean et al., 2015) and by our record at
380 HL (Fig. 5), but site-specific hydrologic conditions could complicate the signals. They may
381 generate inconsistent trends among records over both short (seasonal) and long (millennial)
382 timescales (Gibson et al., 2016; Mark D. Shapley et al., 2008; Steinman & Abbott, 2013; Tyler et
383 al., 2007). Indeed, we observe such inconsistency in the southern Rocky Mountains (Fig. 6).

384 The hydrologic controls, such as groundwater fluxes and basin morphology, can vary
385 based on a lake's geohydrological setting (Anderson et al., 2016; Dean et al., 2015). Modern
386 lake-water hydrogen and oxygen isotope measurements reveal stronger fractionation by
387 evaporation in HL (thick black line, Fig. 2) compared to Bison and Yellow Lakes (purple and



388 yellow lines, Fig. 2), which exhibit a narrower range in modern water isotope values and smaller
389 deviation from the global meteoric water line (Anderson, 2012). However, the carbonate at HL is
390 isotopically lighter than the other two (Fig. 6), which is antithetical to the expectation based on
391 evaporatively enriched summer waters (Fig. 2). The pattern differs from the interpretation that
392 the Bison Lake $\delta^{18}\text{O}_{\text{carb}}$ was not strongly influenced by evaporation because it was isotopically
393 lighter than other sites like Yellow Lake (Anderson, 2011, 2012). HL lacks the prominent
394 $\delta^{18}\text{O}_{\text{carb}}$ trend observed at these other sites (Fig. 6). Given the modern water isotope values, we
395 had anticipated that $\delta^{18}\text{O}_{\text{carb}}$ from HL would be isotopically heavy compared to Bison and
396 Yellow Lakes, but track similar trends (Anderson, 2012).

397 Because the modern water isotope values poorly predicted $\delta^{18}\text{O}_{\text{carb}}$ trends, the different
398 lakes may record past changes in different ways. HL may be a better indicator of winter
399 snowpack than evaporation. $\delta^{18}\text{O}_{\text{carb}}$ values were below the mean at 6 ka (Fig. 5) when simulated
400 estimates of evaporation rates in the Medicine Bow Mountains were up to 30% higher than today
401 (Morrill et al., 2019), which would indicate that such enhanced summer evaporation did not
402 affect $\delta^{18}\text{O}_{\text{carb}}$ at HL. We also find lower-than-expected $\delta^{18}\text{O}_{\text{carb}}$ values in the uppermost
403 sediments. Despite an increase in summer lake-water $\delta^{18}\text{O}$ from -17.8 to -10.8‰ today (thick
404 black line, Fig. 2), $\delta^{18}\text{O}_{\text{carb}}$ values since 1.5 ka only reached a maximum of -16.4‰ and the core-
405 top value is -16.7‰ (Fig. 5), which is closer to the composition of groundwater (open squares,
406 Fig. 2) than the mid- to late-summer lake-water- $\delta^{18}\text{O}$ values (black circles, Fig. 2).

407 Previous studies have shown that the deposition of endogenic carbonate occurs
408 predominantly in the warm summer months when photosynthesis optimizes carbonate production
409 by modifying dissolved CO_2 concentrations and pH (Leng & Marshall, 2004), but the
410 isotopically light carbonate at HL may contradict this expectation. For comparison, the



411 uppermost $\delta^{18}\text{O}_{\text{carb}}$ value of -14.9‰ in Bison Lake (purple line, Fig. 6) falls within the range in
412 modern summer lake-water- $\delta^{18}\text{O}$ values of -16.7 to -13.5‰ (purple line, Fig. 2; Anderson,
413 2011). $\delta^{18}\text{O}_{\text{carb}}$ in HL, therefore, may not integrate the range of summer lake-water $\delta^{18}\text{O}$ as is
414 assumed for Bison and Yellow Lakes (and carbonate lakes in general), but early springtime
415 deposition of carbonate at HL could capture the signature of isotopically light lake water without
416 modification by warm-season evaporation.

417 The year-round measurements of specific conductance show that conditions favorable for
418 carbonate precipitation may indeed be highest during late winter and spring. In 2017, specific
419 conductance of the water below the surface ice rose from 700 $\mu\text{S}/\text{cm}$ in early February to 1,115
420 $\mu\text{S}/\text{cm}$ by early April, and it remained above 1,000 $\mu\text{S}/\text{cm}$ throughout April (Fig. 3). These high
421 values would favor carbonate precipitation, whereas the summertime waters are more dilute.
422 Specific conductance of HL and other lakes within the watershed during the summer typically
423 does not exceed 300 $\mu\text{S}/\text{cm}$. Melting of lake ice and snowpack rapidly lowers the specific
424 conductance by early May and it remains between 250–300 $\mu\text{S}/\text{cm}$ for the remaining ice-free
425 months. The conductance likely remains lower than in winter despite evaporative enrichment of
426 the oxygen isotopes because of groundwater discharge into the lake (Rautio & Korkka-Niemi,
427 2011), which geophysical surveys, water temperatures, and stable summer water levels at HL
428 support (Liefert et al., 2018). If so, ions exsolved from overlying ice raise the conductance of the
429 lake water and pore water within the bottom sediments beyond the concentration in groundwater
430 in winter (Adams & Lasenby, 1985), and create favorable conditions for the rapid deposition of
431 endogenic carbonate in early spring when the isotopic signal would not reflect evaporation or
432 isotopically heavy summer rainfall (open circles, Fig. 2). Spring carbonate formation could also
433 yield a different temperature-dependent effect on the $\delta^{18}\text{O}_{\text{carb}}$ in HL compared to the other lakes,



434 but the cold spring waters at HL should favor an increase, not decrease, in $\delta^{18}\text{O}_{\text{carb}}$. Indeed, all
435 of the readily expected process that could complicate a carbonate isotopic record should drive the
436 $\delta^{18}\text{O}_{\text{carb}}$ in the positive (not negative) direction and underscore the significance of the difference
437 between HL and the other lakes.

438 As an alternative explanation, the $\delta^{18}\text{O}_{\text{carb}}$ values could reflect changes in total
439 precipitation rather than seasonality effects because the inflow of Ca-bearing groundwater
440 (which should rise with precipitation) can increase carbonate production and lower $\delta^{18}\text{O}_{\text{carb}}$
441 values in alkaline lakes in both ice-free and ice-covered conditions (Shapley et al., 2005), but the
442 weak covariance of weight percent carbonate and $\delta^{18}\text{O}_{\text{carb}}$ suggest that rates of groundwater
443 inflow did not strongly influence $\delta^{18}\text{O}_{\text{carb}}$ (Fig. S1a). A weak covariance of $\delta^{13}\text{C}_{\text{carb}}$ and $\delta^{18}\text{O}_{\text{carb}}$
444 indicates short lake-water residence times throughout the lake's history (Fig. S1b; Drummond et
445 al., 1995; Talbot & Kelts, 1990), which could be consistent with rapid flowthrough that reduced
446 evaporative enrichment; removing values from 4.2-4 ka only marginally improves the
447 correlation.

448 A strong negative correlation of weight percent organics and carbonate ($R^2 = -0.79$)
449 suggests that carbonate abundance depends primarily on biological productivity that promoted
450 carbonate dissolution by releasing CO_2 and lowering pH (Fig S1c; Dean, 1999). Carbonate
451 content from 4.2–4 ka was below the mean despite low organic content (red dots, Fig. S1c) and a
452 high flux of carbonate (Fig. 4), which may represent a shift in HL's water levels and chemistry
453 that favored both acidic conditions and isotopically heavy carbonate (red dots, Fig. S1). Down-
454 core shifts in $\delta^{18}\text{O}_{\text{carb}}$ produced by seasonal changes in the timing and rate of carbonate formation
455 have been proposed as potential sources of variability within individual records (Fronval et al.,
456 1995; Lamb et al., 2007; Steinman et al., 2012; Steinman & Abbott, 2013; Tyler et al., 2007) and



457 could play a role in the record at HL, but such differences could also generate the variability in
458 the long-term trends observed among records from the southern Rocky Mountains and elsewhere
459 (Bini et al., 2019; Konecky et al., 2020; Roberts et al., 2008).

460 Other factors that could affect $\delta^{18}\text{O}_{\text{carb}}$, such as precipitation patterns and biological
461 disequilibrium effects, are unlikely sources of variability among the regional $\delta^{18}\text{O}_{\text{carb}}$ records.
462 The seasonal balance of precipitation today is broadly similar among the sites (inset plot, Fig. 2)
463 and the calculated annual precipitation- $\delta^{18}\text{O}$ value is approximately 1‰ lower at HL
464 (<http://waterisotopesDB.org>). Annual temperature ranges are also similar for the watersheds,
465 making it unlikely that temperature dependence of fractionation could explain the range in
466 $\delta^{18}\text{O}_{\text{carb}}$ values recorded across the three records unless the different water depths and
467 groundwater influences altered the seasonal temperature progression among lakes. The
468 difference in temperature would need to be large ($\sim 12\text{ }^{\circ}\text{C}$) to explain the offset in $\delta^{18}\text{O}_{\text{carb}}$
469 between HL and Bison Lake (and larger for the offset between HL and Yellow Lake), which is
470 unrealistic given the sites' comparable locations and elevations and the relatively small
471 temperature changes at mid-latitudes since 11 ka (Marsicek et al., 2018). We also find no
472 evidence in the sediment core or modern lake setting to indicate that biologically mediated
473 precipitation of calcite substantially altered $\delta^{18}\text{O}_{\text{carb}}$ at HL (e.g., by the accumulation of ostracod
474 tests that precipitate carbonates in disequilibrium with lake water). Disequilibrium effects
475 associated with biogenic carbonates generally increase $\delta^{18}\text{O}_{\text{carb}}$ (Holmes & Chivas, 2002; Leng &
476 Marshall, 2004), which would be difficult to reconcile with the surprisingly negative mean and
477 core-top $\delta^{18}\text{O}_{\text{carb}}$ values at HL. Down-core carbonate phase changes are also unlikely as we
478 identified that only calcite was present using x-ray diffraction (XRD).

479



480 6. **Conclusions**

481 $\delta^{18}\text{O}_{\text{carb}}$ from HL indicates an abrupt hydroclimate change in the southern Rocky
482 Mountains from approximately 4.2–4 ka that reduced effective moisture or caused less snow to
483 fall than today at high elevations in southern Wyoming. Other $\delta^{18}\text{O}_{\text{carb}}$ records from the region
484 do not document the drought (Fig. 6; Anderson, 2012), but the event’s timing overlaps with
485 evidence of multi-century drought from pollen, lake stratigraphies, and dunes in the southern
486 Rocky Mountains (Carter et al., 2013; Halfen & Johnson, 2013; Shuman et al., 2009a, 2014,
487 2015; Stokes & Gaylord, 1993), the western Great Plains (Booth et al., 2005; Dean, 1997; Halfen
488 & Johnson, 2013; Mason et al., 1997; Stokes & Gaylord, 1993), and elsewhere around the world
489 (Nakamura et al., 2016; Di Rita & Magri, 2019; Scuderi et al., 2019; Xiao et al., 2018).

490 The timing and magnitude of hydroclimate change in our record agrees with the
491 perspective of a widespread megadrought at around 4.2 ka (Weiss, 2016), but inconsistencies
492 among climate records suggests that (1) site-specific factors can prevent identification of the
493 patterns of abrupt hydroclimate changes, particularly in $\delta^{18}\text{O}_{\text{carb}}$ records; (2) the hydrologic
494 response in North America and likely elsewhere around the world was spatially complex; and (3)
495 the abrupt hydroclimate changes in the North American midcontinent were more pronounced
496 against background Holocene variability than in many regions such as the Atlantic margin.
497 Consequently, a prolonged ‘megadrought’ at 4.2 ka was likely a significant feature of the
498 hydroclimate history in the mid-latitude Rocky Mountains even if that is not true globally.

499

500 **Data availability**

501 Data related to this paper will be made available through the National Centers for Environmental
502 Information on the National Oceanic and Atmospheric Administration website:



503 <https://www.ncdc.noaa.gov/data-access/paleoclimatology-data>. The analyses were performed in

504 R.

505

506 **Author contributions**

507 D. Liefert and B. Shuman contributed to the design and implementation of the research, to the
508 analysis of the results, and to the writing of the manuscript.

509

510 **Acknowledgments**

511 This project was funded by the National Geographic Society (CP-064ER-17), U.S. National
512 Science Foundation P2C2 (EAR-1903729), the Wyoming Center for Environmental Hydrology
513 and Geophysics via support from the U.S. NSF EPSCoR program (EPS-1208909), and the
514 Department of Geology and Geophysics at the University of Wyoming. We thank Andrew
515 Parsekian and Kevin Befus for field assistance and Andrew Flaim for assisting in sample
516 preparation.

517

518 **References**

519 Adams, W. P., & Lasenby, D. C. (1985). The Roles of Snow, Lake Ice and Lake Water in the Distribution of Major
520 Ions in the Ice Cover of a Lake. *Annals of Glaciology*, 7(February 1979), 202–207.

521 <https://doi.org/10.3189/s0260305500006170>

522 Alley, R. B., Mayewski, P. A., Sowers, T., Stuiver, M., Taylor, K. C., & Clark, P. U. (1997). Holocene climatic
523 instability: A prominent, widespread event 8200 yr ago. *Geology*, 25(6), 483–486.

524 [https://doi.org/10.1130/0091-7613\(1997\)025<0483:HCIAPW>2.3.CO;2](https://doi.org/10.1130/0091-7613(1997)025<0483:HCIAPW>2.3.CO;2)

525 Anderson, L. (2011). Holocene record of precipitation seasonality from lake calcite $\delta^{18}O$ in the central Rocky
526 Mountains, United States. *Geology*, 39(3), 211–214. <https://doi.org/10.1130/G31575.1>

527 Anderson, L. (2012). Rocky Mountain hydroclimate: Holocene variability and the role of insolation, ENSO, and the
528 North American Monsoon. *Global and Planetary Change*, 92–93, 198–208.



- 529 <https://doi.org/10.1016/j.gloplacha.2012.05.012>
- 530 Anderson, L., Berkelhammer, M., Barron, J. A., Steinman, B. A., Finney, B. P., & Abbott, M. B. (2016a). Lake
531 oxygen isotopes as recorders of North American Rocky Mountain hydroclimate: Holocene patterns and
532 variability at multi-decadal to millennial time scales. *Global and Planetary Change*, 137, 131–148.
533 <https://doi.org/10.1016/j.gloplacha.2015.12.021>
- 534 Anderson, L., Berkelhammer, M., Barron, J. A., Steinman, B. A., Finney, B. P., & Abbott, M. B. (2016b). Lake
535 oxygen isotopes as recorders of North American Rocky Mountain hydroclimate: Holocene patterns and
536 variability at multi-decadal to millennial time scales. *Global and Planetary Change*, 137, 131–148.
537 <https://doi.org/10.1016/j.gloplacha.2015.12.021>
- 538 Anderson, R. S., Allen, C. D., Toney, J. L., Jass, R. B., & Bair, A. N. (2008). Holocene vegetation and fire regimes
539 in subalpine and mixed conifer forests, southern Rocky Mountains, USA. *International Journal of Wildland
540 Fire*, 17(1), 96. <https://doi.org/10.1071/WF07028>
- 541 Arz, H. W., Lamy, F., & Pätzold, J. (2006). A pronounced dry event recorded around 4.2 ka in brine sediments from
542 the northern Red Sea. *Quaternary Research*, 66(3), 432–441. <https://doi.org/10.1016/j.yqres.2006.05.006>
- 543 Ault, T. R., George, S. S., Smerdon, J. E., Coats, S., Mankin, J. S., Carrillo, C. M., et al. (2018). A robust null
544 hypothesis for the potential causes of megadrought in Western North America. *Journal of Climate*, 31(1), 3–
545 24. <https://doi.org/10.1175/JCLI-D-17-0154.1>
- 546 Bello, R., & Smith, J. D. (1990). The Effect of Weather Variability on the Energy Balance of a Lake in the Hudson
547 Bay Lowlands, Canada. *INSTAAR, University of Colorado*, 22(1), 98–107.
- 548 Bini, M., Zanchetta, G., Perşoiu, A., Cartier, R., Català, A., Cacho, I., et al. (2019). The 4.2 ka BP Event in the
549 Mediterranean region: An overview. *Climate of the Past*, 15(2), 555–577. [https://doi.org/10.5194/cp-15-555-
550 2019](https://doi.org/10.5194/cp-15-555-2019)
- 551 Booth, R. K., Jackson, S. T., Forman, S. L., Kutzbach, J. E., Bettis, E. A., Kreig, J., & Wright, D. K. (2005). A
552 severe centennial-scale drought in mid-continental North America 4200 years ago and apparent global
553 linkages. *Holocene*, 15(3), 321–328. <https://doi.org/10.1191/0959683605hl825ft>
- 554 Bradley, R. S., & Bakke, J. (2019). Is there evidence for a 4.2 ka BP event in the northern North Atlantic region?
555 *Climate of the Past*, 15(5), 1665–1676. <https://doi.org/10.5194/cp-15-1665-2019>
- 556 Brunelle, A., Minckley, T. A., Lips, E., & Burnett, P. (2013). A record of Lateglacial/Holocene environmental



- 557 change from a high-elevation site in the Intermountain West, USA. *Journal of Quaternary Science*, 28(1),
558 103–112. <https://doi.org/10.1002/jqs.2600>
- 559 Carter, V. A., Brunelle, A., Minckley, T. A., Dennison, P. E., & Power, M. J. (2013). Regionalization of fire regimes
560 in the Central Rocky Mountains, USA. *Quaternary Research (United States)*, 80(3), 406–416.
561 <https://doi.org/10.1016/j.yqres.2013.07.009>
- 562 Carter, V. A., Shinker, J. J., & Preece, J. (2018). Drought and vegetation change in the central Rocky Mountains and
563 western Great Plains: Potential climatic mechanisms associated with megadrought conditions at 4200 cal yr
564 BP. *Climate of the Past*, 14(8), 1195–1212. <https://doi.org/10.5194/cp-14-1195-2018>
- 565 Clark, P. U., Webb, R. S., & Keigwin, L. D. (1999). *Mechanisms of global climate change at millennial time scales*.
566 Washington, DC: American Geophysical Union.
- 567 Dean, J. R., Jones, M. D., Leng, M. J., Noble, S. R., Metcalfe, S. E., Sloane, H. J., et al. (2015). Eastern
568 Mediterranean hydroclimate over the late glacial and Holocene, reconstructed from the sediments of Nar lake,
569 central Turkey, using stable isotopes and carbonate mineralogy. *Quaternary Science Reviews*, 124, 162–174.
570 <https://doi.org/10.1016/j.quascirev.2015.07.023>
- 571 Dean, W. E. (1997). Rates, timing, and cyclicity of Holocene eolian activity in north-central United States: Evidence
572 from varved lake sediments. *Geology*, 25(4), 331–334. [https://doi.org/10.1130/0091-7613\(1997\)025<0331:RTACOH>2.3.CO;2](https://doi.org/10.1130/0091-7613(1997)025<0331:RTACOH>2.3.CO;2)
- 573 Dean, W. E. (1999). The carbon cycle and biogeochemical dynamics in lake sediments. *Journal of Paleolimnology*,
574 21(4), 375–393. <https://doi.org/10.1023/A:1008066118210>
- 575 Deininger, M., McDermott, F., Mudelsee, M., Werner, M., Frank, N., & Mangini, A. (2017). Coherency of late
576 Holocene European speleothem $\delta^{18}O$ records linked to North Atlantic Ocean circulation. *Climate Dynamics*,
577 49(1–2), 595–618. <https://doi.org/10.1007/s00382-016-3360-8>
- 578
- 579 Denniston, R. F., Gonzalez, L. A., Baker, R. G., Asmerom, Y., Reagan, M. K., Edwards, R. L., & Alexander, E. C.
580 (1992). Speleothem evidence for Holocene fluctuations of the prairie-forest ecotone, 6, 671–676.
- 581 Drummond, C. N., Patterson, W. P., & Walker, J. C. G. (1995). Climatic forcing of carbon-oxygen isotopic
582 covariance in temperate-region marl lakes. *Geology*, 23(11), 1031. [https://doi.org/10.1130/0091-7613\(1995\)023<1031:cfocoi>2.3.co;2](https://doi.org/10.1130/0091-7613(1995)023<1031:cfocoi>2.3.co;2)
- 583
- 584 Feiler, E. J., Scott, R., & Koehler, A. (2017). Late Quaternary Paleoenvironments of the White River Plateau ,



- 585 Colorado, U. S. A. Author(s): Eric J. Feiler, R. Scott Anderson and Peter A. Koehler Published by :
586 INSTAAR, University of Colorado Stable URL : <http://www.jstor.org/stable/1551836>, 29(1), 53–62.
- 587 Forman, S. L., Oglesby, R., & Webb, R. S. (2001). Temporal and spatial patterns of Holocene dune activity on the
588 Great Plains of North America: Megadroughts and climate links. *Global and Planetary Change*, 29(1–2), 1–
589 29. [https://doi.org/10.1016/S0921-8181\(00\)00092-8](https://doi.org/10.1016/S0921-8181(00)00092-8)
- 590 Fronval, T., Jensen, N. B., & Buchardt, B. (1995). Oxygen isotope disequilibrium precipitation of calcite in Lake
591 Arreso, Denmark. *Geology*, 23(5), 463–466. [https://doi.org/10.1130/0091-
592 7613\(1995\)023<0463:OIDPOC>2.3.CO;2](https://doi.org/10.1130/0091-7613(1995)023<0463:OIDPOC>2.3.CO;2)
- 593 Gibson, J. J., Birks, S. J., Yi, Y., Moncur, M. C., & McEachern, P. M. (2016). Stable isotope mass balance of fifty
594 lakes in central Alberta: Assessing the role of water balance parameters in determining trophic status and lake
595 level. *Journal of Hydrology: Regional Studies*, 6, 13–25. <https://doi.org/10.1016/j.ejrh.2016.01.034>
- 596 Von Grafenstein, U., Erlenkeuser, H., Müller, J., Jouzel, J., & Johnsen, S. (1998). The cold event 8200 years ago
597 documented in oxygen isotope records of precipitation in Europe and Greenland. *Climate Dynamics*, 14(2),
598 73–81. <https://doi.org/10.1007/s003820050210>
- 599 Halfen, A. F., & Johnson, W. C. (2013). A review of Great Plains dune field chronologies. *Aeolian Research*, 10,
600 135–160. <https://doi.org/10.1016/j.aeolia.2013.03.001>
- 601 Halfen, A. F., Fredlund, G. G., & Mahan, S. A. (2010). Holocene stratigraphy and chronology of the Casper Dune
602 Field, Casper, Wyoming, USA. *Holocene*, 20(5), 773–783. <https://doi.org/10.1177/0959683610362812>
- 603 Henderson, A. K., & Shuman, B. N. (2009). Hydrogen and oxygen isotopic compositions of lake water in the
604 western United States. *Geological Society of America Bulletin*, 121(7–8), 1179–1189.
605 <https://doi.org/10.1130/B26441.1>
- 606 Holmes, J. A., & Chivas, A. R. (2002). Ostracod shell chemistry—overview. *Geophysical Union Geophysical
607 Monograph Series*, 131, 185–204.
- 608 Houston, R. S., & Karlstrom, K. E. (1992). Geologic map of Precambrian metasedimentary rocks of the Medicine
609 Bow Mountains, Albany and Carbon counties, Wyoming. *U.S. Geological Survey Miscellaneous
610 Investigations Map*, I-2280. Sc.
- 611 Huang, C. C., Pang, J., Zha, X., Su, H., & Jia, Y. (2011). Extraordinary floods related to the climatic event at 4200 a
612 BP on the Qishuihe River, middle reaches of the Yellow River, China. *Quaternary Science Reviews*, 30(3–4),



- 613 460–468. <https://doi.org/10.1016/j.quascirev.2010.12.007>
- 614 Jalali, B., Sicre, M. A., Azuara, J., Pellichero, V., & Combourieu-Nebout, N. (2019). Influence of the North Atlantic
615 subpolar gyre circulation on the 4.2 ka BP event. *Climate of the Past*, 15(2), 701–711.
616 <https://doi.org/10.5194/cp-15-701-2019>
- 617 Jiménez-Moreno, G., Anderson, R. S., Shuman, B. N., & Yackulic, E. (2019). Forest and lake dynamics in response
618 to temperature, North American monsoon and ENSO variability during the Holocene in Colorado (USA).
619 *Quaternary Science Reviews*, 211, 59–72. <https://doi.org/10.1016/j.quascirev.2019.03.013>
- 620 Johnson, B. G., Jiménez-Moreno, G., Eppes, M. C., Diemer, J. A., & Stone, J. R. (2013). A multiproxy record of
621 postglacial climate variability from a shallowing, 12-m deep sub-alpine bog in the southeastern San Juan
622 Mountains of Colorado, USA. *The Holocene*, 23(7), 1028–1038. <https://doi.org/10.1177/0959683613479682>
- 623 Kahle, D., & Wickham, H. (2013). ggmap: Spatial Visualization with ggplot2. *The R Journal*, 5(1), 144–161.
- 624 Konecky, B. L., McKay, N. P., Sidorova, O. V. C., Comas-bru, L., Dassié, P., Delong, K. L., et al. (2020). The Iso2k
625 Database: A global compilation of paleo- $\delta^{18}\text{O}$ and $\delta^2\text{H}$ records to aid understanding of Common Era climate.
626 *Earth Syst. Sci. Data Discuss.*, (In review). Retrieved from <https://doi.org/10.5194/essd-2020-5>
- 627 Lamb, H. F., Leng, M. J., Telford, R. J., Ayenew, T., & Umer, M. (2007). Oxygen and carbon isotope composition
628 of authigenic carbonate from an Ethiopian lake: A climate record of the last 2000 years. *Holocene*, 17(4), 517–
629 526. <https://doi.org/10.1177/0959683607076452>
- 630 Leng, M. J., & Marshall, J. D. (2004). Palaeoclimate interpretation of stable isotope data from lake sediment
631 archives. *Quaternary Science Reviews*, 23(7–8), 811–831. <https://doi.org/10.1016/j.quascirev.2003.06.012>
- 632 Li, Y. X., Yu, Z., & Kodama, K. P. (2007). Sensitive moisture response to Holocene millennial-scale climate
633 variations in the Mid-Atlantic region, USA. *Holocene*, 17(1), 3–8. <https://doi.org/10.1177/0959683606069386>
- 634 Liefert, D. T., Shuman, B. N., Parsekian, A. D., & Mercer, J. J. (2018). Why Are Some Rocky Mountain Lakes
635 Ephemeral? *Water Resources Research*, 54(8), 5245–5263. <https://doi.org/10.1029/2017WR022261>
- 636 Marsicek, J., Shuman, B. N., Bartlein, P. J., Shafer, S. L., & Brewer, S. (2018). Reconciling divergent trends and
637 millennial variations in Holocene temperatures. *Nature*, 554(7690), 92–96.
638 <https://doi.org/10.1038/nature25464>
- 639 Marsicek, J. P., Shuman, B., Brewer, S., Foster, D. R., & Oswald, W. W. (2013). Moisture and temperature changes
640 associated with the mid-Holocene Tsuga decline in the northeastern United States. *Quaternary Science*



- 641 *Reviews*, 80, 129–142. <https://doi.org/10.1016/j.quascirev.2013.09.001>
- 642 Mason, J. P., Swinehart, J. B., & Loope, D. B. (1997). Holocene history of lacustrine and marsh sediments in a
643 dune-blocked drainage, Southwestern Nebraska Sand Hills, U.S.A. *Journal of Paleolimnology*, 17(1), 67–83.
644 <https://doi.org/10.1023/A:1007917110965>
- 645 Mayewski, P. A., Rohling, E. E., Stager, J. C., Karlén, W., Maasch, K. A., Meeker, L. D., et al. (2004). Holocene
646 climate variability. *Quaternary Research*, 62(3), 243–255. <https://doi.org/10.1016/j.yqres.2004.07.001>
- 647 Mensing, S., Korfmacher, J., Minckley, T., & Musselman, R. (2012). A 15,000 year record of vegetation and
648 climate change from a treeline lake in the Rocky Mountains, Wyoming, USA. *The Holocene*, 22(7), 739–748.
649 <https://doi.org/10.1177/0959683611430339>
- 650 Minckley, T. A., Shriver, R. K., & Shuman, B. (2012). Resilience and regime change in a southern Rocky Mountain
651 ecosystem during the past 17000 years TL - 82. *Ecological Monographs*, 82 VN-r(1), 49–68.
652 <https://doi.org/10.1890/11-0283.1>
- 653 Mock, C. . (1996). Climate controls and spatial variations of precipitation in the western United States. *Journal of*
654 *Climate*, 9, 1111–1125.
- 655 Morrill, C., Meador, E., Livneh, B., Liefert, D. T., & Shuman, B. N. (2019). Quantitative model-data comparison of
656 mid-Holocene lake-level change in the central Rocky Mountains. *Climate Dynamics*, 0(0), 0.
657 <https://doi.org/10.1007/s00382-019-04633-3>
- 658 Musselman, R. C., Connell, B. H., Conrad, M. A., Dufford, R. G., Fox, D. G., Haines, J. D., et al. (1992). The
659 Glacier Lakes Ecosystem Experiments Site.
- 660 Nakamura, A., Yokoyama, Y., Maemoku, H., Yagi, H., Okamura, M., Matsuoka, H., et al. (2016). Weak monsoon
661 event at 4.2 ka recorded in sediment from Lake Rara, Himalayas. *Quaternary International*, 397, 349–359.
662 <https://doi.org/10.1016/j.quaint.2015.05.053>
- 663 Newby, P. E., Shuman, B. N., Donnelly, J. P., Karnauskas, K. B., & Marsicek, J. (2014). Centennial-to-millennial
664 hydrologic trends and variability along the North Atlantic Coast, USA, during the Holocene. *Geophysical*
665 *Research Letters*, 41(12), 4300–4307. <https://doi.org/10.1002/2014GL060183>
- 666 Nolan, C. (2020). *Using Co-Located Lake and Bog Records to Improve Inferences on Late Quaternary Climate and*
667 *Ecology*.
- 668 Parnell, A. C., Haslett, J., Allen, J. R. M., Buck, C. E., & Huntley, B. (2008). A flexible approach to assessing



- 669 synchronicity of past events using Bayesian reconstructions of sedimentation history. *Quaternary Science*
670 *Reviews*, 27(19–20), 1872–1885. <https://doi.org/10.1016/j.quascirev.2008.07.009>
- 671 Preece, J. R., Shinker, J. J., Riebe, C. S., & Minckley, T. A. (2020). Elevation-dependent precipitation response to El
672 Niño-Southern oscillation revealed in headwater basins of the US central Rocky Mountains. *International*
673 *Journal of Climatology*, (November 2019), 1–12. <https://doi.org/10.1002/joc.6790>
- 674 Railsback, L. B., Liang, F., Brook, G. A., Voarintsoa, N. R. G., Sletten, H. R., Marais, E., et al. (2018). The timing,
675 two-pulsed nature, and variable climatic expression of the 4.2 ka event: A review and new high-resolution
676 stalagmite data from Namibia. *Quaternary Science Reviews*, 186, 78–90.
677 <https://doi.org/10.1016/j.quascirev.2018.02.015>
- 678 Ran, M., & Chen, L. (2019). The 4.2 ka BP climatic event and its cultural responses. *Quaternary International*,
679 (April), 0–1. <https://doi.org/10.1016/j.quaint.2019.05.030>
- 680 Rautio, A., & Korkka-Niemi, K. (2011). Characterization of groundwater-lake water interactions at Pyhäjärvi, a lake
681 in SW Finland. *Boreal Environment Research*, 16(5), 363–380.
- 682 Renssen, H., Goosse, H., & Muscheler, R. (2006). Coupled climate model simulation of Holocene cooling events:
683 oceanic feedback amplifies solar forcing, 79–90.
- 684 Di Rita, F., & Magri, D. (2019). The 4.2 ka event in the vegetation record of the central Mediterranean. *Climate of*
685 *the Past*, 15(1), 237–251. <https://doi.org/10.5194/cp-15-237-2019>
- 686 Roberts, N., Jones, M. D., Benkaddour, A., Eastwood, W. J., Filippi, M. L., Frogley, M. R., et al. (2008). Stable
687 isotope records of Late Quaternary climate and hydrology from Mediterranean lakes: the ISOMED synthesis.
688 *Quaternary Science Reviews*. <https://doi.org/10.1016/j.quascirev.2008.09.005>
- 689 Roland, T. P., Caseldine, C. J., Charman, D. J., Turney, C. S. M., & Amesbury, M. J. (2014). Was there a “4.2ka
690 event” in Great Britain and Ireland? Evidence from the peatland record. *Quaternary Science Reviews*, 83, 11–
691 27. <https://doi.org/10.1016/j.quascirev.2013.10.024>
- 692 Rosenberry, D. O., & LaBaugh, J. W. (2008). *Field Techniques for Estimating Water Fluxes Between Surface Water*
693 *and Ground Water*. <https://doi.org/10.3133/tm4D2>
- 694 Scuderi, L. A., Yang, X., Ascoli, S. E., & Li, H. (2019). The 4.2 ka BP Event in northeastern China: A geospatial
695 perspective. *Climate of the Past*, 15(1), 367–375. <https://doi.org/10.5194/cp-15-367-2019>
- 696 Shapley, M. D., Ito, E., & Donovan, J. J. (2005). Authigenic calcium carbonate flux in groundwater-controlled



- 697 lakes: Implications for lacustrine paleoclimate records. *Geochimica et Cosmochimica Acta*, 69(10), 2517–
698 2533. <https://doi.org/10.1016/j.gca.2004.12.001>
- 699 Shapley, Mark D., Ito, E., & Donovan, J. J. (2008). Isotopic evolution and climate paleorecords: Modeling boundary
700 effects in groundwater-dominated lakes. *Journal of Paleolimnology*, 39(1), 17–33.
701 <https://doi.org/10.1007/s10933-007-9092-3>
- 702 Shinker, J. J. (2010). Visualizing spatial heterogeneity of western U.S. climate variability. *Earth Interactions*,
703 14(10). <https://doi.org/10.1175/2010EI323.1>
- 704 Shuman, B., Henderson, A. K., Colman, S. M., Stone, J. R., Fritz, S. C., Stevens, L. R., et al. (2009). Holocene lake-
705 level trends in the Rocky Mountains, U.S.A. *Quaternary Science Reviews*, 28(19–20), 1861–1879.
706 <https://doi.org/10.1016/j.quascirev.2009.03.003>
- 707 Shuman, B., Pribyl, P., Minckley, T. A., & Shinker, J. J. (2010). Rapid hydrologic shifts and prolonged droughts in
708 Rocky Mountain headwaters during the Holocene. *Geophysical Research Letters*.
709 <https://doi.org/10.1029/2009GL042196>
- 710 Shuman, B. N., & Burrell, S. A. (2017). Centennial to millennial hydroclimatic fluctuations in the humid northeast
711 United States during the Holocene. *Quaternary Research (United States)*, 88(3), 514–524.
712 <https://doi.org/10.1017/qua.2017.62>
- 713 Shuman, B. N., Carter, G. E., Hougardy, D. D., Powers, K., & Shinker, J. J. (2014). A north-south moisture dipole at
714 multi-century scales in the Central and Southern Rocky Mountains, U.S.A., during the late Holocene. *Rocky
715 Mountain Geology*, 49(1), 33–49. <https://doi.org/10.2113/gsrocky.49.1.33>
- 716 Shuman, B. N., Pribyl, P., & Buettner, J. (2015). Hydrologic changes in Colorado during the mid-Holocene and
717 Younger Dryas. *Quaternary Research (United States)*, 84(2), 187–199.
718 <https://doi.org/10.1016/j.yqres.2015.07.004>
- 719 Shuman, B. N., Marsicek, J., Oswald, W. W., & Foster, D. R. (2019). Predictable hydrological and ecological
720 responses to Holocene North Atlantic variability. *Proceedings of the National Academy of Sciences of the
721 United States of America*, 116(13), 5985–5990. <https://doi.org/10.1073/pnas.1814307116>
- 722 Steinman, B. A., & Abbott, M. B. (2013). Isotopic and hydrologic responses of small, closed lakes to climate
723 variability: Hydroclimate reconstructions from lake sediment oxygen isotope records and mass balance
724 models. *Geochimica et Cosmochimica Acta*. <https://doi.org/10.1016/j.gca.2012.11.027>



- 725 Steinman, B. A., Abbott, M. B., Nelson, D. B., Stansell, N. D., Finney, B. P., Bain, D. J., & Rosenmeier, M. F.
726 (2012). Isotopic and hydrologic responses of small, closed lakes to climate variability: Comparison of
727 measured and modeled lake level and sediment core oxygen isotope records. *Geochimica et Cosmochimica*
728 *Acta*, 105, 455–471. <https://doi.org/10.1016/j.gca.2012.11.026>
- 729 Stewart, R. B., & Rouse, W. R. (1976). A Simple Method for Determining the Evaporation From Shallow Lakes and
730 Ponds. *Water Resources Research*, 12(4), 623–628. <https://doi.org/10.1029/WR012i004p00623>
- 731 Stokes, S., & Gaylord, D. R. (1993). Optical Dating of Holocene Dune Sands in the Ferris Dune Field, Wyoming.
732 *Quaternary Research*, 39, 274–281.
- 733 Talbot, M. R. (1990). A review of the palaeohydrological interpretation of carbon and oxygen isotopic ratios in
734 primary lacustrine carbonates. *Chemical Geology (Isotope Geosci. Sect.)*, 80, 261–279.
- 735 Talbot, M. R., & Kelts, K. (1990). Paleolimnological signatures from carbon and oxygen isotopic ratios in
736 carbonates from organic-rich lacustrine sediments. *Lacustrine Exploration: Case Studies and Modern*
737 *Analogs*, 99–112.
- 738 Thompson, R. S., Whitlock, C., Bartlein, P. J., Harrison, S. P., Geoffrey Spaulding, W. (1993). Climatic Changes in
739 the Western United States since 18,000 yr B.P. In P. J. Wright, Jr., H. E., Kutzbach, J. E., Webb III, T.,
740 Ruddiman, W. F., Street-Perrott, F. A., Bartlein (Ed.), *Global Climates since the Last Glacial Maximum* (pp.
741 468–513). University of Minnesota Press.
- 742 Tyler, J. J., Leng, M. J., & Arrowsmith, C. (2007). Seasonality and the isotope hydrology of Lochnagar, a Scottish
743 mountain lake: Implications for palaeoclimate research. *Holocene*, 17(6), 717–727.
744 <https://doi.org/10.1177/0959683607080513>
- 745 Walker, M., Gibbard, P., Head, M. J., Berkelhammer, M., Björck, S., Cheng, H., et al. (2019). Formal Subdivision
746 of the Holocene Series/Epoch: A Summary. *Journal of the Geological Society of India*, 93(2), 135–141.
747 <https://doi.org/10.1007/s12594-019-1141-9>
- 748 Wanner, H., Wanner, H., Mercolli, L., Mercolli, L., Grosjean, M., Grosjean, M., & Ritz, S. P. (2015). Holocene
749 climate variability and change; a data-based review. *Journal of the Geological Society*, 172(2), 254–263.
750 <https://doi.org/10.1144/jgs2013-101>
- 751 Wanner, Heinz, Beer, J., Bütikofer, J., Crowley, T. J., Cubasch, U., Flückiger, J., et al. (2008). Mid- to Late
752 Holocene climate change: an overview. *Quaternary Science Reviews*, 27(19–20), 1791–1828.



- 753 <https://doi.org/10.1016/j.quascirev.2008.06.013>
- 754 Wanner, Heinz, Solomina, O., Grosjean, M., Ritz, S. P., & Jetel, M. (2011). Structure and origin of Holocene cold
755 events. *Quaternary Science Reviews*, 30(21–22), 3109–3123. <https://doi.org/10.1016/j.quascirev.2011.07.010>
- 756 Weiss, H. (2016). Climate change and cultural evolution across the world. *Past Global Change Magazine*, 24(2),
757 62–63. <https://doi.org/10.22498/pages.24.2.55>
- 758 Weiss, H. (2019). Interactive comment on “ Is there evidence for a 4 . 2 ka BP event in the northern North Atlantic
759 region ?” by Raymond Bradley and Jostein Bakke. *Climate of the Past Discussions*.
760 <https://doi.org/https://doi.org/10.5194/cp-2018-162-RC2>, 2019
- 761 Whitlock, C., & Bartlein, P. J. (1993). Spatial Variations of Holocene Climatic Change in the Yellowstone Region.
762 *Quaternary Research*, 39, 231–238.
- 763 Wise, E. K. (2010). Spatiotemporal variability of the precipitation dipole transition zone in the western United
764 States. *Geophysical Research Letters*, 37(7), n/a-n/a. <https://doi.org/10.1029/2009gl042193>
- 765 Xiao, J., Zhang, S., Fan, J., Wen, R., Zhai, D., Tian, Z., & Jiang, D. (2018). The 4.2 ka BP event:
766 Multi-proxy records from a closed lake in the northern margin of the East Asian summer monsoon. *Climate of*
767 *the Past*, 14(10), 1417–1425. <https://doi.org/10.5194/cp-14-1417-2018>
- 768 Yan, M., & Liu, J. (2019). Physical processes of cooling and mega-drought during the 4.2 ka BP event: Results from
769 TraCE-21ka simulations. *Climate of the Past*, 15(1), 265–277. <https://doi.org/10.5194/cp-15-265-2019>
- 770 Zhang, H., Cheng, H., Cai, Y., Spötl, C., Kathayat, G., Sinha, A., et al. (2018). Hydroclimatic variations in
771 southeastern China during the 4.2 ka event reflected by stalagmite records. *Climate of the Past*,
772 14(11), 1805–1817. <https://doi.org/10.5194/cp-14-1805-2018>
- 773 Zhu, C., Lettenmaier, D. P., & Cavazos, T. (2005). Role of antecedent land surface conditions on North American
774 monsoon rainfall variability. *Journal of Climate*, 18(16), 3104–3121. <https://doi.org/10.1175/JCLI3387.1>
775